JB
Journals.ASM.org

A Genetic Screen in *Myxococcus xanthus* Identifies Mutants That Uncouple Outer Membrane Exchange from a Downstream Cellular Response

Arup Dey, Daniel Wall

Department of Molecular Biology, University of Wyoming, Laramie, Wyoming, USA

Upon physical contact with sibling cells, myxobacteria transiently fuse their outer membranes (OMs) and exchange OM proteins and lipids. From previous work, TraA and TraB were identified to be essential factors for OM exchange (OME) in donor and recipient cells. To define the genetic complexity of OME, we carried out a comprehensive forward genetic screen. The screen was based on the observation that *Myxococcus xanthus* nonmotile cells, by a Tra-dependent mechanism, block swarm expansion of motile cells when mixed. Thus, mutants defective in OME or a downstream responsive pathway were readily identified as escape flares from mixed inocula seeded on agar. This screen was surprisingly powerful, as we found >50 mutants defective in OME. Importantly, all of the mutations mapped to the *traAB* operon, suggesting that there may be few, if any, proteins besides TraA and TraB directly required for OME. We also found a second and phenotypically different class of mutants that exhibited wild-type OME but were defective in a responsive pathway. This pathway is postulated to control inner membrane homeostasis by covalently attaching amino acids to phospholipids. The identified proteins are homologous to the *Staphylococcus aureus* MprF protein, which is involved in membrane adaptation and antibiotic resistance. Interestingly, we also found that a small number of nonmotile cells were sufficient to block the swarming behavior of a large gliding-proficient population. This result suggests that an OME-derived signal could be amplified from a few nonmotile producers to act on many responder cells.

Myxobacteria are Gram-negative gliding bacteria that exhibit complex social behaviors. One of these interesting behaviors is their ability to transiently fuse their outer membranes (OMs) and exchange contents (1). The exchange of OM material can be visualized in live cells with fluorescent protein reporters fused to an OM lipoprotein signal sequence or by use of fluorescent OM lipids (2, 3). Phenotypically, OM exchange (OME) can be monitored by extracellular complementation between certain motility mutants. In this assay, a small subset of gliding mutants is transiently rescued or stimulated by the transfer of missing motility proteins from a donor strain that contains the corresponding wild-type protein (4, 5). For stimulation to occur, the cargo protein must reside in the OM, as cytoplasmic and inner membrane proteins are not transferred (2). Because *Myxococcus xanthus* expresses >400 lipoproteins (6), OME between cells probably involves hundreds of different OM proteins and, consequently, is likely to affect a variety of cellular processes (2). Although the function of OME in wild-type cells is not fully understood, it may play a role in establishing envelope homeostasis and cell-cell communication and may generally assist in the transition from individual cells to coherent multicellular populations (7).

To investigate the mechanism and biological function of OME, we sought to identify cellular factors required for OME. To do this, in a prior study, we characterized a historic mutant derived from the Kaiser Laboratory strain collection (3). This heretofore uncharacterized nonmotile mutant (DK396) was of interest because it universally failed to stimulate all six classes of *cgl* and *tgl* motility mutants (4, 8, 9), whose protein products function in adventurous (A)- and social (S)-gliding motility, respectively (for reviews, see references 10 to 12). The genome of this strain was sequenced, and the causative mutation was identified in a gene that we named *traA*. Interestingly, TraA function is required in both the donor and recipient strains, suggesting that OM transfer is bidirectional. Subsequently, we found that the downstream gene in the bicistronic operon, *traB*, is also required for OME (3). Immunolocalization studies showed that TraA localizes on the cell surface, with a tendency to reside near the cell poles (13). Phylogenetic and molecular analyses indicated that TraA functions as a homotypic cell surface receptor/adhesin that recognizes other cells bearing identical or similar TraA alleles (13). Thus, the intimate cellular process of sharing OM contents occurs only between siblings or cells that bear a nearly identical *traA* allele. Molecular recognition within and between species is determined by a polymorphic domain (PA14-like) within TraA. The specific function of TraB is unknown, but it is likely to interact with TraA (3).

In this study, we sought to conduct the first forward genetic screen to define the total complement of proteins involved in OME. This screen was based on the finding that nonmotile mutants block swarm expansion of motile strains by a Tra-dependent mechanism when mixed together (3, 13). To understand the basis of the screen, it is important to recognize that swarm inhibition is distinct from stimulation; the former blocks wild-type motility, and the latter rescues the motility of certain mutants (4). Although the mechanism of swarm inhibition is not well understood, it is thought to involve a signal that is generated from the physiological state of the nonmotile cells, as swarm inhibition initiates after a

Received 14 August 2014 **Accepted** 22 September 2014
Published ahead of print 29 September 2014
Address correspondence to Daniel Wall, dwall2@uwyo.edu.
Supplemental material for this article may be found at http://dx.doi.org/10.1128/JB.02217-14.

doi:10.1128/JB.02217-14

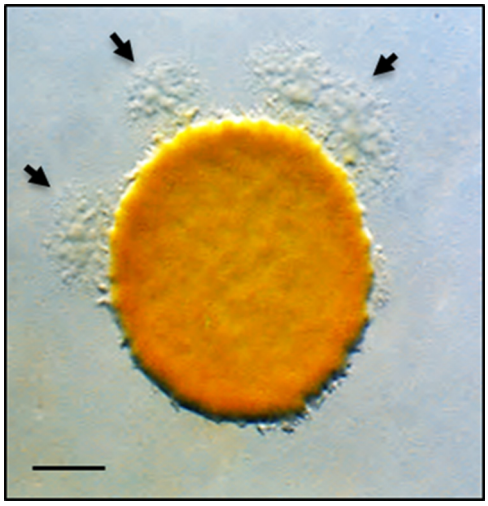

FIG 1 Micrograph showing how escape flare mutants were identified. A nonmotile strain was mixed at a 1:1 ratio with an A-motile strain that was mutagenized with a transposon (representing a pool of mutagenized genomes). After 5 days of incubation, escape flares (arrows) are readily seen. Bar, 1 mm.

1-day incubation on agar surfaces (3, 14). In contrast, stimulation primarily occurs during the first day of incubation and subsides in subsequent days; thus, there appears to be a temporal switch for when stimulation or swarm inhibition can occur. Stimulation and swarm inhibition are similar in the sense that both require cell-cell contact, a hard agar surface, and TraAB function. Here, we exploited the swarm inhibition phenotype as a means to identify mutants defective in OME. In this regard, mutants were easily identified because they resulted in the production of escape flares derived from the motile strain (Fig. 1). The second goal of this work was to identify downstream factors or a pathway(s) that responds to cell-cell interactions mediated by OME. Mutants that affect these factors or this pathway(s) should undergo normal OME but exhibit a relief of swarm inhibition phenotype, because they are defective in perceiving or responding to OME.

MATERIALS AND METHODS

Strains and media. The bacterial strains used in the study are listed in Table 1 (15, 16). *M. xanthus* was grown in the dark at 33°C in CTT medium (1% Casitone, 10 mM Tris-HCl [pH 7.6], 8 mM $MgSO_4$, 1 mM KH_2PO_4) without or with kanamycin (Km; 50 μg/ml), as needed. In the genetic screen and in stimulation assays, 1/2 CTT plates, where the Casitone concentration was reduced to 0.5% and 2 mM $CaCl_2$ was added with 1.5% agar, were used. To generate time-lapse movies of motility, 1/4 CTT 0.8% agarose pads (no $CaCl_2$) were made on glass slides. To make the media, either tap or filter purified water was used. For routine cloning, *Escherichia coli* DH5α *pir*$^+$ was grown at 37°C in LB medium with 50 μg/ml Km.

Genetic screen. The pMini-Himar-*lacZ* transposon, pRL27 (17), and EZ-Tn*5* (Epicentre) were transformed into *M. xanthus* (DK8615 or DK10410) using standard protocols (18) (Table 1). After electroporation, the cells were allowed to recover by shaking at 33°C for 5 to 6 h. After ~6 days of incubation, the colonies from each transformant plate were pooled, and the cell density of each pool was concentrated to ~1.5×10^9 CFU/ml. A nonmotile *M. xanthus* strain (DK8601) was also grown and prepared to a similar cell density. Each individual mutant pool and DK8601 were mixed at equal volumes, and about a dozen 5-μl aliquots were pipetted onto 1/2 CTT Omni (Nunc) agar plates with 2 mM $CaCl_2$. The plates were incubated at 33°C and observed for emergent flares after 3 to 5 days. Cells from these flares were collected with a sterile toothpick and transferred onto fresh CTT-Km plates. To verify mutant phenotypes, purified isolates were grown to 3×10^8 CFU/ml and mixed at a 1:1 ratio with DK8601, and aliquots were pipetted onto agar plates. After 2 days of incubation, the spots were visually inspected for emergent flares.

To sequence transposon insertions from *M. xanthus*, genomic DNA was isolated with an UltraClean microbial DNA isolation kit (MO BIO Laboratories, Inc.) and digested with restriction enzymes (pMini-Himar-*lacZ* and mini-Tn*5*, SacII; EZ-Tn*5*, EcoRI, HindIII, or SalI; New England BioLabs). The digested DNA was ligated with T4 DNA ligase (New England BioLabs) and transformed into *E. coli*. Candidate clones were then isolated, and in the case of pMini-Himar-*lacZ*, derived clones were analyzed by diagnostic MluI restriction digestion. Plasmid DNA was sequenced at the University of Wyoming Macromolecular Analysis Core facility with appropriately named primers, which are described in Table 1.

Strain construction. To backcross transposon insertions into different strains, generalized transduction was done with bacteriophage Mx8. In-frame gene deletion constructs for MXAN_4427 and MXAN_4428 were made using a Gibson cloning strategy (New England BioLabs), wherein PCR products were ligated with the pBJ114 plasmid (19). Restriction-verified plasmids were then electroporated into *M. xanthus* and plated on CTT-Km plates. Transformants were grown in the absence of Km and then counterselected on CTT plates with 2% galactose. In-frame deletion mutants were confirmed by PCR using primers flanking the deletion (Table 1). Gene disruptions were made using internal gene fragments that were PCR amplified and ligated into the pCR2.1 TOPO XL vector (Table 1). Restriction-verified clones were then transformed into *M. xanthus* and selected for on CTT-Km plates.

Microbial assays. To test for protein transfer, cells were grown and concentrated to 3×10^9 CFU/ml in TPM buffer (10 mM Tris-HCl [pH 7.6], 8 mM $MgSO_4$, 1 mM KH_2PO_4). The cells were then mixed with a nonmotile double-labeled DW1056 strain (in which the cytoplasm was labeled with green fluorescent protein [GFP_{Cyto}] and the OM was labeled with an mCherry reporter fused to a signal sequence [SS_{OM}-mCherry]) at a 1:1 ratio. Aliquots of the mixture (5 μl each) were transferred to TPM buffer–0.8% agarose pads and incubated in a humid chamber. After 6 h, the cells were observed by phase-contrast and fluorescence microscopy with a ×20 objective lens for the presence of SS_{OM}-mCherry in the emergent flares (2). In addition, transfer was evaluated with a 100× oil immersion lens. Here mutants that express GFP (recipient) were grown and concentrated as described above. These cells were then mixed with donor *M. xanthus* cells expressing SS_{OM}-mCherry, and the cell mixture was placed on a TPM buffer plate at a 1:5 ratio (recipient/donor) and incubated in a humid chamber for 2 h. The cells were then collected, washed twice with TPM buffer, and observed on a glass slide. Micrographs were obtained with a phase-contrast/fluorescence microscope that was coupled to digital imaging systems, as described previously (2).

Stimulation tests were done by mixing a strain that is nonmotile but stimulatable (DW1466 Δ*cglC tgl*::Tc) with various nonmotile donor mutants at a 1:1 ratio and then transferring the cells to 1/2 CTT agar plates with 2 mM $CaCl_2$. To monitor A-gliding motility, the cell density was measured, and cells were concentrated to 1.5×10^9 CFU/ml and placed on 1/2 CTT with 1.5% agar and 2 mM $CaCl_2$. To monitor S-gliding motility, the cells were concentrated as described above and pipetted onto semisolid (0.5% agar) CTT plates with 2 mM $MgSO_4$.

RESULTS

Genetic screen. To define the OME gene set, we conducted a genetic screen in *M. xanthus*. Initially, a pilot transposon-based screen was done for donor mutants defective in stimulation. Although this strategy was feasible, we encountered two problems. First, the screen was laborious. Second, mutants which initially appeared to be defective in stimulation based on a cross-streak assay against a stimulatable strain were subsequently found to be false positive, when a more sensitive culture-based assay was used

TABLE 1 Strains, plasmids, and primers

Strain, plasmid, or primer	Relevant features or sequence	Source or reference
Strains		
DH5α *pir*$^+$	*E. coli* cloning strain	Lab collection
DK1217	A$^-$ S$^+$ *aglB1*	13
DK8601	A$^-$ S$^-$ *aglB1* Δ*pilA*::Tc Tc^r	12
DK8606	A$^-$ S$^-$ *aglB1* Δ*pilA* P_{pilA}-*gfp* Km^r	12
DK8615	A$^+$ S$^-$ Δ*pilQ*	13
DK10410	A$^+$ S$^-$ Δ*pilA*	12
DW709	DK10410 Δ*pilA* P_{pilA}-*gfp* Km^r	28
DW1056	DK8606 P_{pilA}-SS_{OM}-mCherry(pXW6) P_{pilA}-*gfp* Sm^r Tc^r Km^r	2
DW1415	DK8615 *traA*::pDP2 Km^r	3
DW1466	A$^-$ S$^-$ Δ*cglC* Δ*tgl*::Tc Tc^r	3
DW1467	DK8601 *aglB1* Δ*traA* Δ*pilA*::Tc Tc^r	11
DW1478	DK8615 P_{pilA}-SS_{OM}-mCherry(pXW6) Sm^r	This study
DW1479	DW1478 *traA*::pDP2 Km^r Sm^r	This study
DW1601	DK8615 *omrA*::EZ-Tn*5* Km^r	This study
DW1602	DK8615 *omrA*::mini-Himar-*lacZ* Km^r	This study
DW1603	DK8615 *omrA*::mini-Tn*5* Km^r	This study
DW1604	DK8601 *aglB1* Δ*pilA*::Tc *omrA*::mini-Tn*5* Tc^r Km^r	This study
DW1605	DK1217 *omrA*::mini-Tn*5* Km^r	This study
DW1606	DK8615 Δ*phpA* (markerless)	This study
DW1607	DK1217 Δ*phpA* (markerless)	This study
DW1608	DK8615 ΔMXAN_4428 (markerless)	This study
DW1609	DK8615 *omrB*::pAD3 Km^r Zm^r	This study
DW1610	DK8601 *omrB*::pAD3 Km^r Zm^r	This study
DW1611	DW1603 P_{pilA}-SS_{OM}-mCherry(pXW6) Sm^r Km^r	This study
DW1612	DW1466 *omrA*::mini-Tn*5* Km^r Tc^r	This study
Plasmids		
pMini-Himar-*lacZ*	*mariner*-derived transposon with *lacZ oriR6K*, Km^r	Heidi Kaplan
pRL27	Mini-Tn*5* *oriR6K* hyperactive transposase, Km^r	14
pCR2.1 TOPO XL	Cloning vector, Km^r Zm^r	Life Technologies
pCR2.1 TOPO TA	Cloning vector, Km^r	Life Technologies
pDP2	*traA* (insertion cassette) in pCR2.1 TOPO TA, Km^r	3
pDP21	P_{pilA}-RBS_{syn}-*traAB* cloned in pSWU1, Km^r	3
pXW6	P_{pilA}-SS_{OM}-mCherry cassette cloned in pKSAT, Sm^r	2
pAD1	Δ*phpA* cassette in pBJ114, Km^r	This study
pAD2	ΔMXAN_4428 cassette in pBJ114, Km^r	This study
pAD3	*omrB* (insertion cassette) in pCR2.1 TOPO XL, Km^r Zm^r	This study
Primers		
Mariner primer	TGTGTTTTTCTTTGTTAGACCG	
EZ-Tn*5* KAN-2 Fwd	ACCTACAACAAAGCTCTCATCAACC	
EZ-Tn*5* KAN-2 Rev	GCAATGTAACATCAGAGATTTTGAG	
Tpn RL13 (mini-Tn*5*)	CAGCAACACCTTCTTCACGA	
Tpn RL17 (mini-Tn*5*)	AACAAGCCAGGGATGTAACG	
MXAN_4428delupstrfwd	TATGACCATGATTACGCCAAGCTTAGGTTCACCTCGGTGGC	
MXAN_4428delupstrrev	ATCCCAGCGCTGTGAAGCTGTGTGGATGGGACACGTCAGGGT	
MXAN_4428deldwnstrfwd	CACACAGCTTCACAGCGCTGGGATGCACGCCAGCACGGCGAC	
MXAN_4428deldwnstrrev	CGTTGTAAAACGACGGCCAGTGAATTCCCTCATGAGACGGGCGAAGC	
MXAN_4427delupstrfwd	TATGACCATGATTACGCCAAGCTTCTCTCGCTCGTGGGTGAC	
MXAN_4427delupstrrev	CCAGCGCTGTGAAGCTGTGTGGCAATGCAGGTCGACAAAG	
MXAN_4427deldwnstrfwd	CACACAGCTTCACAGCGCTGGAATCCCGCGACTTTGTTG	
MXAN_4427deldwnstrrev	CGTTGTAAAACGACGGCCAGTGAATTCAGTACAGCGCCGTGTAGAGG	
MXAN_6818 KO FWD	GGACAGACGGTGTTCTCGTT	
MXAN_6818 KO REV	ACAGGAAGCCCACCACCT	

(see below), at a problematically high frequency. The false positives appeared to stem from undefined physiological differences among isolates that arose during screening. On the basis of these outcomes, a different approach was sought.

As described above, in a prior study we discovered that OME can regulate the swarming behavior of *M. xanthus* cells that are proficient for gliding motility (3). Specifically, when a nonmotile strain, which also could not be stimulated, was mixed at a 1:1 ratio with a motile strain, the ability of the motile strain to swarm was significantly impaired. Importantly, swarm inhibition was re-

lieved when either the motile or nonmotile strain contained a mutation in *traA* or *traB*. When the *tra* mutation was in the motile strain, the swarm rate of the motile strain was fully restored, as if the nonmotile strain elicited no inhibitory effect (see below). In contrast, when the *tra* mutation was in the nonmotile strain, there was a partial restoration of swarming (3). Additionally, when inhibited swarms were incubated for extended periods, e.g., 7 to 10 days, escape flares were typically found (data not shown). When cells from these flares were isolated and retested, swarm expansion usually ensued when they were mixed with a nonmotile strain, indicating that these isolates contained suppressors that had spontaneously developed. Finally, for reasons that are unknown, OME-dependent swarm inhibition primarily acted on the A-motility system (data not shown).

Based on the above findings, we reasoned that an A-motile strain could be mutagenized and mutant pools could then be mixed with a nonmotile strain to screen for escape flare mutants. Such escape mutants were expected to be defective in OME or in a downstream pathway in the responder cell (an A-motile strain) that no longer responds to OME. To allow facile gene identification and to help ensure a wide distribution of mutations, three different transposons were used: one was *mariner* based, and two were Tn*5* based. Using this strategy, nine separate screens, each consisting of 2,000 to 3,000 mutants, were conducted, resulting in ~20,000 total transposon mutants being screened. To conduct this screen, the cells in the initial transformation plates, which each contained 200 to 400 transposon mutants, were individually pooled, their cell densities were measured, and the cells were then mixed at a 1:1 ratio with a nonmotile strain. In total, about 80 unique mutant pools were screened. Figure 1 shows a representative example of how escape flares were identified.

To help avoid the isolation of spontaneous mutations, escape flares were identified 3 to 5 days after plating. Cells from identified flares were then isolated and retested for a relief of swarm inhibition. This effort yielded 75 mutants that recapitulated the relief of swarm inhibition phenotype after purification. The genomic insertion sites for all 75 transposon mutants were determined and resulted in the identification of 33 genes. Of these, 30 genes were hit only once and 3 genes were hit multiple times. To test if the mutations bred true, a representative mutation from each gene was backcrossed into a parental strain (DK8615). Interestingly, none of the single-hit genes bred true or the phenotype in the resulting transductants could not be confirmed as a bona fide swarm relief. In contrast, all three of the genes that were hit multiple times bred true.

For 2 of the 30 single-hit genes that did not breed true but did exhibit a full swarm relief phenotype in the original mutants (both of which were derived from *mariner* mutagenesis), we investigated possible explanations for the genetic discrepancies. In these two cases, the mutant strains where found by PCR analysis to have a second transposon insertion in *traA*, thus accounting for their phenotypes (data not shown). The occurrence of multiple *mariner* transposon insertions within single mutant strains is in agreement with the findings of a prior study by Hartzell and coworkers (18). For the remaining 28 single-hit mutants, all of which exhibited only a partial swarm expansion phenotype (see below), we concluded that those strains were likely to contain secondary mutations, either spontaneous or transposon based, or the phenotypes were too subtle to be detected after the backcross. In any case, these mutants were not further studied.

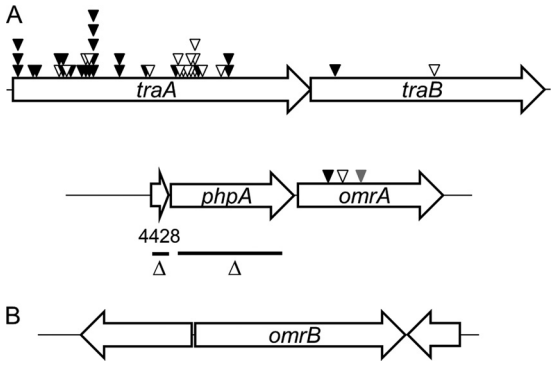

FIG 2 Genetic maps of discovered genes. (A) Transposon insertions isolated in *traA* (MXAN_6895), *traB* (MXAN_6898), and *omrA* (MXAN_4426) are shown. Black, white, and gray triangles, *mariner*, Tn*5*, and EZ-Tn*5* transposon insertions, respectively. In-frame deletion (Δ) regions in *phpA* (MXAN_4427) and MXAN_4428 are indicated as black bars. (B) Genetic organization of the *omrB* (MXAN_6818) locus. Genes are drawn approximately to scale.

As shown in Fig. 2A, *traA* was hit 40 times (or 42 times when the 2 mutants described above are included) in this screen, whereas *traB* was hit twice. These results validate the screen, as over half of the mutations isolated were in genes known to be required for OME and swarm inhibition. Of the 40 sequenced transposon insertions within *traA*, 31 were clearly from independent isolates (16 from *mariner* and 15 from Tn*5* derived from pRL27), because their insertion sites differed or they were isolated from independent mutagenesis screens. The remaining nine *traA* insertions could represent sibling clones because the insertions were in the same position and derived from the same mutagenesis screen as the other mutants. The three remaining transposon insertions were in a new gene (MXAN_4426) that we named *omrA* (OME response A) (Fig. 2A).

Finally, to help ensure that the screen was comprehensive, we isolated spontaneous and UV-induced mutants that similarly produced escape flares. This effort yielded 15 additional mutants that were confirmed upon retesting. From complementation studies, where a *traAB*-containing plasmid (pDP21) was transformed into these mutant strains, 11 additional mutations were mapped to the *traAB* locus (data not shown). The mutations in the remaining four strains were not mapped.

The OME response can be amplified by a minority cell population to control behaviors in large populations. Although the three *omrA* mutants relieved swarm inhibition, their phenotypes were partial compared to the full relief seen with *traA* or *traB* mutants. To help quantify phenotypic differences, the ratio of motile to nonmotile cells was varied. Surprisingly, in the control mixture, a ratio of one nonmotile cell to 40 (or even 50) motile cells resulted in complete swarm inhibition, i.e., inhibition was similar to that at a 1:1 ratio or a reversed 40:1 ratio (Fig. 3, second row, and data not shown). Importantly, this result indicates that a small number of nonmotile cells block the swarm expansion of many cells.

As discussed above, swarm inhibition requires OME, as a *tra* mutant A-motile strain could swarm equally well whether alone or mixed with nonmotile cells at ratios of 40:1, 1:1, or 1:40 (Fig. 3; compare row 1 to row 3; note that when the motile population was high [1:40 ratio], swarm expansion was the largest). For the *omrA*

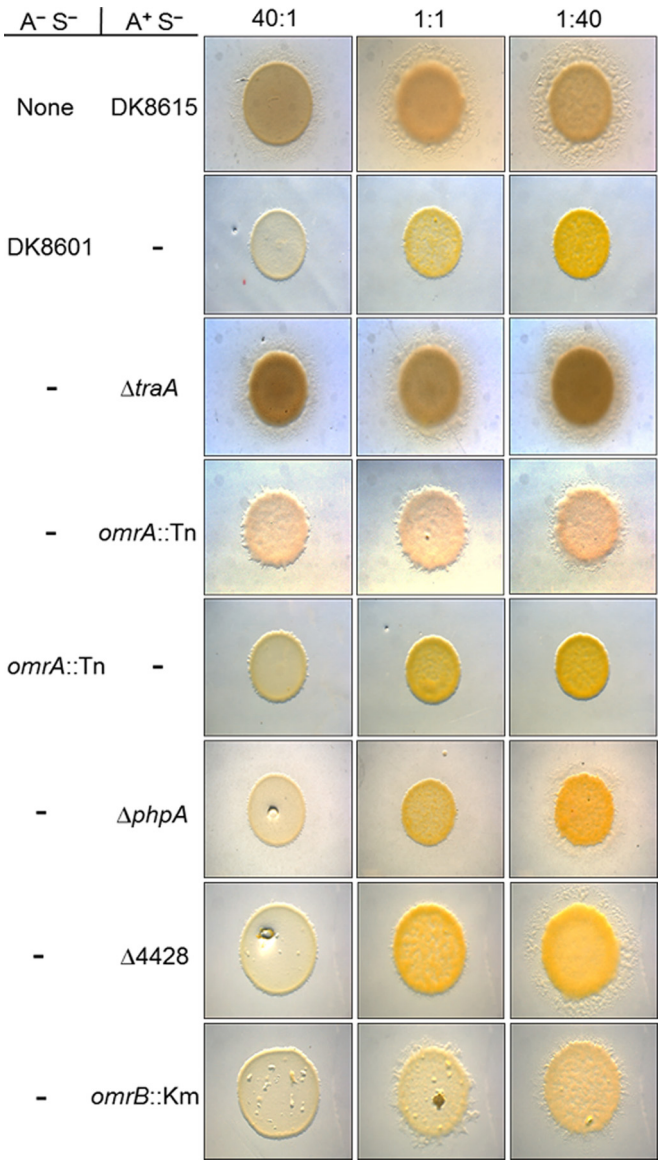

FIG 3 OME and the response pathway regulate swarm expansion of mixed strains. Nonmotile (A^- S^-) and A-motile (A^+ S^-) strains were mixed at the ratios indicated at the top and incubated for 3 days. The top row is a control where the A-motile strain DK8615 was instead mixed with buffer. All rows below contain strain mixtures; in rows that contain a parental strain (DK8601 or DK8615), the strain is identified by a dash, and in rows that contain derivative strains, the mutations are indicated. The strains are listed in Table 1.

mutant, there was a relief of swarm inhibition at all three ratios, although at all ratios the phenotype was partial, meaning that the swarm areas for the *traA* mutant mixtures or A-motility monocultures were greater (Fig. 3; compare row 4 to rows 3 and 1). From a temporal analysis, the swarm relief phenotypes of the *traA* and *omrA* mutants were difficult to visually discern at day 1 or 2 and required a compound microscope to do so; however, by day 3 their phenotypic differences were apparent (Fig. 3 and data not shown).

To examine individual cell motility dynamics, time-lapse movies were made of strain mixtures. As reported previously (3), when a nonmotile strain was mixed with an A-motile strain, the cellular movements of the latter strain significantly decreased or stopped after 1 day of incubation, whereas isogenic *traA* mutants continued to glide (compare Movies S1 and S2 in the supplemental material; time point, 72 h). Similar to a *traA* mutant, the *omrA* mutant retained gliding movements after a 72-h incubation with the nonmotile strain (DK8601), although the movements of the *traA* mutant were more robust than those of the *omrA* mutant (compare Movies S2 and S3 in the supplemental material). In addition, by 96 h incubation with DK8601, the relative motility of the *omrA* mutant stopped, while the *traA* mutant retained motility (data not shown). Therefore, the full swarm relief phenotype of a mixed *traA* colony (Fig. 3) can be explained by the sustained and unobstructed cell movements seen by time-lapse microscopy. Similarly, the partial swarm relief phenotype of a mixed *omrA* colony correlates with reduced cell movements, which subside after a 3-day incubation.

OmrA is not required for OME. TraA and TraB are required in both donor and recipient cells for OME and swarm inhibition (3). To test whether OmrA functions similarly in donor strains, the *omrA* mutation was introduced into a nonmotile strain (DK8601). In contrast to what was found in an A-motile strain background, when the nonmotile strain contained the *omrA*::mini-Tn*5* mutation (DW1604), complete swarm inhibition was observed at all strain ratios (Fig. 3, fifth row). Importantly, this result indicates that OmrA plays a role only in responder cells and demonstrates a function distinct from that of TraA and TraB.

To determine whether OmrA is required for OME, we carried out a stimulation assay. Here, a nonmotile donor strain that contained the *omrA*::mini-Tn*5* allele (DW1604) was mixed with a nonmotile strain (DW1466 Δ*cglC* Δ*tgl*::Tc) that can be stimulated for both A- and S-motility by OME (3). The nonmotile *omrA* mutant stimulated DW1466 to glide, whereas the *traA* mutant did not (Fig. 4A). Compared with the stimulation by the Tra^+ parental control, stimulation by the *omrA* mutant was notably and reproducibly impaired (Fig. 4A); however, the significance of the reduced stimulation is not clear, because we have found that other mutants, as well as medium conditions or the physiological state of cells, can similarly impair stimulation (3, 20) (data not shown). In addition, the *omrA*::mini-Tn*5* allele was also introduced into the DW1466 recipient strain, and in this genetic background, stimulation occurred at wild-type levels (Fig. 4A). These results indicate that unlike the *traA* or *traB* mutation, the *omrA* mutation still allows the CglC and Tgl proteins to be transferred.

The *omrA* mutant was directly tested for transfer of the OM lipoprotein reporter (SS_{OM}-mCherry). As described previously (2), these experiments were conducted by mixing and incubating an SS_{OM}-mCherry donor with a GFP-labeled recipient. Here, the recipient strain contained GFP in the cytoplasm, where it cannot be transferred (2). OME was thus scored as green recipients turning red or yellow in the merged fluorescence micrographs. The *omrA* mutant efficiently transferred SS_{OM}-mCherry, as the GFP recipient became red (Fig. 4B). Compared with the OME in the positive control, no defect in OME was observed, whereas a *traA* mutant donor was not able to transfer SS_{OM}-mCherry (Fig. 4B). From these results, we conclude that OmrA is not required for OME but instead plays a role in perceiving or responding to OME (TraAB function).

Genetic characterization of the *omrA* operon. *omrA* resides as the distal gene in an apparent operon with two upstream genes (Fig. 2A), suggesting that these gene products could function to-

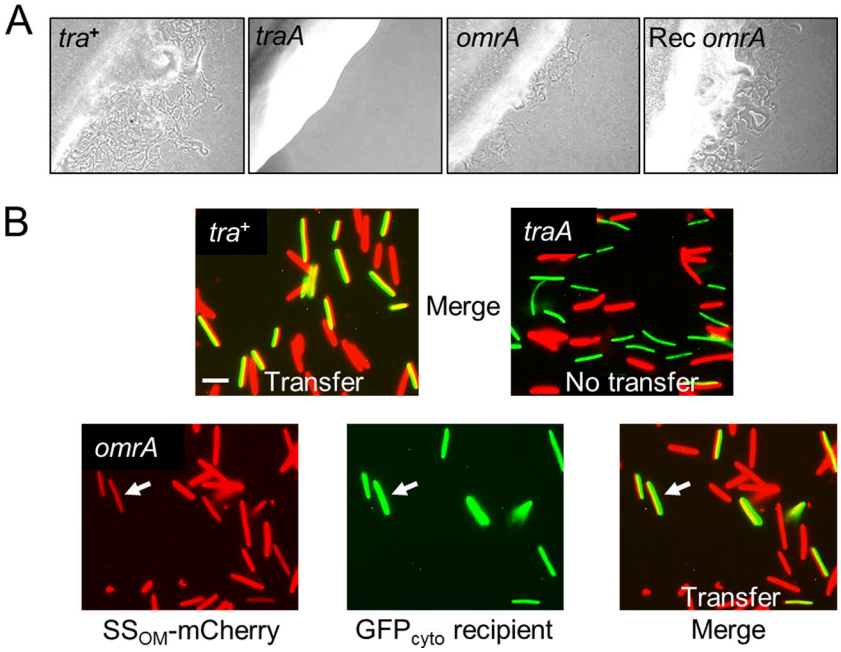

FIG 4 OmrA is not required for stimulation or lipoprotein transfer. (A) A nonmotile but stimulatable recipient (DW1466) was mixed with isogenic nonmotile donors that contain the indicated alleles (DK8601, DW1467, and DW1604 in the first, second, and third panels, respectively). In the far right panel, the stimulatable recipient (Rec) instead contains the *omrA* mutation (DW1612 mixed with DK8601). Micrographs were taken after 1 day of incubation. (B) (Top) Merged fluorescence micrographs showing that transfer (yellow) of the SS_{OM}-mCherry lipoprotein to a GFP-labeled recipient (DW709) is Tra dependent (DW1478, *tra*$^+$; DW1479, *traA* mutant). Bar, 3 μm. (Bottom) Lipoprotein transfer from an isogenic *omrA*::mini-Tn*5* donor (DW1611). To show the transfer unambiguously, the red, green, and merged panels are all shown. Arrows, transfer to a recipient cell.

gether in a biological pathway. To address this possibility, in-frame and markerless deletion mutations were created in the upstream genes (Fig. 2A) in an A-motile (DK8615) background. These mutants, the ΔMXAN_4428 and Δ*phpA* (ΔMXAN_4427) mutants, were then tested for swarm inhibition. As shown in rows 6 and 7 of Fig. 3, these mutants exhibited a relief of swarm inhibition when mixed at a 1:40 (nonmotile cell-to-motile cell) ratio but not when mixed with higher ratios of nonmotile cells. Additionally, we noted that the swarm expansion was variable even at the 1:40 ratio, as cells often initially emerged as isolated flares, instead of as a continuous swarm front, which subsequently encased the inoculum spot (data not shown). The significance of this modest relief of swarm inhibition is unclear, as the parental strain (DK8615) did expand when the mixed strain ratio was reduced to 1:80 (data not shown). Thus, in this swarm assay, the ΔMXAN_4428 and Δ*phpA* mutations resulted in a 2-fold increase, at best, in the ratio of nonmotile cells. Finally, we note that these partial or poor swarm relief phenotypes would not have been detected under our stringent screening conditions (1:1 ratio).

The PhpA protein has been biochemically shown to function as a tyrosine phosphatase and, in a physiological context, is involved in exopolysaccharide (EPS) regulation, because a *phpA* mutant overexpresses EPS (21). Because EPS is required for S-motility (22), we tested the Δ*phpA* mutant for S-motility defects in a strain that lacks A-motility (A^-). The Δ*phpA* strain had reduced S-motility on semisolid agar, a medium that favors S-motility (23), and the colony center was composed of macroscopic cell aggregates (see Fig. S1A in the supplemental material). Under the same conditions, an *omrA* mutant also had reduced S-motility; however, its colony morphology was similar to that of the parental strain (see Fig. S1A in the supplemental material). When the Δ*phpA* mutation was placed in the A^+ S^- genetic background (DW1606), a reduced-A-motility phenotype was also observed, but no macroscopic aggregates were detected (see Fig. S1B in the supplemental material). In contrast, cells in the same background with *omrA* or ΔMXAN_4428 mutations exhibited wild-type A-motility (data not shown). Upon microscopic examination, Δ*phpA* cells were found to clump in solution, and in an S-motility-positive (S^+) background, the cell clumps could become large (compare Fig. S1C to D in the supplemental material). In support of these findings, Kimura and colleagues reported that a Δ*phpA* mutant has a hyperagglutination phenotype (21).

The Δ*phpA* and ΔMXAN_4428 mutants revealed no growth defect phenotypes, whereas *omrA* mutants showed several poor growth phenotypes. First, *omrA* mutants grew slowly, and, second, the cultures stopped growing at a mid-log-phase cell density of ~2×10^8 CFU/ml (~70 Klett units). However, when the shaker flasks were incubated for extended periods, the culture turbidity of the *omrA* mutants eventually increased, suggesting that suppressors had developed. In support of this conclusion, when an *omrA* mutant culture was subsequently propagated, the cultures exhibited no growth defects; however, the swarm relief phenotype was retained. Last, reviving naive *omrA* mutants from −80°C freezer stocks proved difficult and in some cases was not possible. Consequently, fresh mutants were constructed by transductions, and transductants were immediately used in the described experiments.

Bioinformatic analysis identifies OmrB. The OmrA protein has significant sequence homology to Pfam PF03706 (UPF0104) (E value, 1.7e−38). The best-characterized PF03706 family mem-

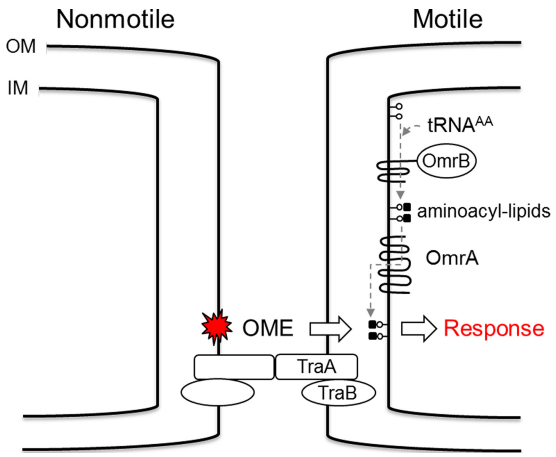

FIG 5 Working model for how OmrA and OmrB modulate the OME response. Here, aminoacylation of phospholipids and transfer to the outer leaflet of the inner membrane allow an undefined OME-derived signal (red star) to be perceived by a responder cell. Lollipops, phospholipids. See the text for additional details. IM, inner membrane; AA, aminoacyl.

ber is MprF from *Staphylococcus aureus*, where this domain resides in the cytoplasmic membrane and has phospholipid flippase activity (24). Consistent with a PF03706 designation, OmrA, like other family members, was predicted to contain eight transmembrane helices (TMHMM, version 2.0) (25) (Fig. 5). Within the Pfam database (July 2014) (26), PF03706 was most frequently found as a single-domain protein (3,567 homologs); its second most frequent protein form consisted of an architecture where PF03706 was fused to a domain called DUF2156 (PF09924; 962 homologs), as found in MprF (24). To investigate whether other proteins may function in an OmrA pathway, we searched the *M. xanthus* DK1622 genome for ORFs that contained PF09924 (27). From this search a single gene (MXAN_6818) that contained a domain with significant homology to PF09924 (E value, 1.1e−40) was identified. To test whether this gene functions in an OME response pathway, we created a gene disruption in MXAN_6818. Interestingly, the mutant (DW1609) showed a partial relief of swarm inhibition when mixed at 1:1 and 1:40 ratios of nonmotile to motile cells (Fig. 3, bottom row). Because the MXAN_6818 disruption mutant exhibited a partial swarm relief phenotype and was competent for OME (data not shown), similar to *omrA* mutants, the gene was designated *omrB*. However, we emphasize that at a 40:1 ratio the *omrB*::Km mutant showed complete swarm inhibition, whereas at this ratio the *omrA*::mini-Tn*5* mutant retained partial swarm expansion (Fig. 3), which suggests that the *omrA* mutant has a more pronounced swarm relief phenotype. As shown in Fig. 2B, *omrB* is monocistronic in the DK1622 genome.

The function of MXAN_4428 remains unknown, although the gene product shows significant homology to PF03884 (DUF329; E value, 1e−18), a domain which belongs to the TRASH clan, a family of small proteins that contain conserved cysteine residues thought to bind metal ions (28). In *E. coli*, YacG, a PF03884 family member, binds GyrB and inhibits DNA gyrase activity (29).

DISCUSSION

In this work, we describe a powerful genetic screen that allowed isolation of *M. xanthus* mutants defective in OME. In total, 44 transposon mutants with mutations in *traA* and *traB* were isolated, and additional point mutations were mapped to this locus. Because no other genes were found to be required for OME, we conclude that the protein machinery directly involved in OM fusion is relatively simple and likely consists of only TraA and TraB in partnering cells. Consistent with this view, in available myxobacterial genomes, the *traAB* genes are always found in an operon by themselves (30). Furthermore, in other bacterial systems that transport effectors into neighboring cells, namely, type III, IV, V, and VI secretion systems, the genes that encode the transport apparatus are also found to be contained in operons or genetic islands (31–33). In eukaryotes, where membrane fusion systems are better understood, they typically consist of one to a few proteins essential for fusion (34). Thus, on the basis of *a priori* evidence and our screen, the TraAB proteins may be sufficient to explain OM fusion in myxobacteria. Moreover, as no mutants were found to be defective in the production of OM tubes, which are long narrow outer membrane-enclosed cellular appendages (35), these or other overt cellular structures appear to not be required for OME, as previously suggested (35, 36).

The ease with which *traAB* mutants were isolated suggests that the screen provided a powerful fitness advantage to A-motile cells when OME was abolished. One obvious fitness gain is the ability of motile cells to escape captivity from nonmotile siblings. Here, escape mutants can seek fresh nutrients and leave crowded areas that contain metabolic wastes. However, given the lopsided outcomes, other fitness gains that are currently not appreciated may be endowed to *tra* escape mutants.

Our screen yielded a second class of mutants that were fully competent for OME. These mutants were instead defective for the OME response. A working model for the OME response pathway is outlined in Fig. 5. Importantly, because the swarm relief phenotype of the *omr* mutants was not as robust as that of the *tra* mutants (Fig. 3), the former mutant class was more difficult to isolate. Consequently, we expect the OME response pathway(s) to consist of additional players that have not yet been identified.

The swarm inhibition phenotype described here cannot be explained simply as a physical obstruction by nonmotile cells, because cells with *tra* mutations alleviate this block. To explain swarm inhibition, our model proposes that a time-dependent physiological signal or cue is generated in nonmotile cells and is then transmitted to motile cells (Fig. 5). In this model, OME either directly transfers an inhibitory signal or the TraAB function acts as a cue that triggers signal transfer by an undefined mechanism. Consistent with a signaling hypothesis, our findings that a few nonmotile cells can control the gliding behavior of a large population (Fig. 3, 1:40 ratio) can be explained by a mechanism whereby a signal is amplified and propagated from one to many cells. Because our screen pertained to motile responders, signal-generating mutants could not be obtained and the nature of the putative signal(s) remains unknown. Last, our findings from strain mixture experiments suggest that cells within myxobacterial swarms are communicating and cell behaviors are regulated. We hypothesize that the introduction of nonmotile cells within a motile population breaks the harmony of the population and leads to swarm dysfunction. Consistent with this view, Kaiser and Warrick have recently demonstrated that the movement of cells within a swarm shows a surprisingly high degree of synchronization (37). We suggest that this synchronization is disrupted when nonmotile cells are mixed in the population.

Insights into how cells respond to OME can be gleaned from

the literature on OmrA and OmrB homologs. In particular, MprF from *S. aureus* represents a model protein. MprF is a bifunctional enzyme that contains a natural fusion between the domains found in OmrA and OmrB (24). The MprF PF09924 domain (OmrB) catalyzes the synthesis of lysyl-phosphatidylglycerol from lysyl-tRNA and phosphatidylglycerol precursors. The resulting membrane-embedded aminoacyl-phosphatidylglycerol is then flipped from the cytoplasmic membrane leaflet to the outside leaflet by domain PF03706 (OmrA). Within family members, the aminoacyl-phosphatidylglycerol synthases and flippase functions can be promiscuous with respect to substrates containing lysine, alanine, and/or arginine (38–40). Aminoacylation of phosphatidylglycerol in turn results in physicochemical changes in the cytoplasmic membrane and how it interacts with molecules. For example, in *S. aureus*, gain-of-function mutations in MprF result in antibiotic resistance, including resistance to daptomycin, by altering the membrane surface charge, which in turn repels cationic antibiotics (24). Peschel and colleagues have shown that the two domains in MprF can be genetically separated and yet their functions are retained (41). By analogy to MprF and the PA0920 homolog in *Pseudomonas aeruginosa* (39), we propose that OmrB similarly functions to aminoacylate phospholipids on the inner leaflet of the cytoplasmic membrane (Fig. 5). Although aminoacylated phosphatidylglycerol has not yet been reported in *M. xanthus*, this field is an emerging area of research in which bacteria have been found to adapt to their environments by modifying their phospholipids (42). Additionally, it is known that *M. xanthus* contains chemically diverse phospholipids (43), and MprF homologs in the *M. xanthus* genome have also been reported by others (44). We propose that, after amino acid addition to phosphatidylglycerol, OmrA flips this substrate to the outer leaflet of the inner membrane (Fig. 5). In support of this model, the finding that both *omrA* and *omrB* mutants elicit a swarm relief phenotype (Fig. 3) provides genetic evidence that these proteins function in the same pathway. However, we emphasize that at a high ratio of nonmotile cells, the *omrB* mutant did not elicit swarm relief, while the *omrA* mutant did (Fig. 3), suggesting that OmrA plays a more critical role in the responsive pathway. In turn, we suggest that *omrA* or *omrB* mutations alter membrane homeostasis, and, consequently, the physiological response of responder cells to OME engagement changes. Possible cellular scenarios to explain an altered response include how effector proteins, small molecules, and/or toxins interact with the inner membrane and/or proteins therein. Currently, we are investigating the molecular details for how cells respond to OME to coordinate multicellular behaviors.

ACKNOWLEDGMENTS

We thank Bill Metcalf for pRL27 and Trish Hartzell for pMini-Himar-*lacZ*.

This work was supported by NIH grant GM101449 to D.W.

REFERENCES

1. **Nudleman E, Wall D, Kaiser D.** 2005. Cell-to-cell transfer of bacterial outer membrane lipoproteins. Science **309:**125–127. http://dx.doi.org/10.1126/science.1112440.
2. **Wei X, Pathak DT, Wall D.** 2011. Heterologous protein transfer within structured myxobacteria biofilms. Mol. Microbiol. **81:**315–326. http://dx.doi.org/10.1111/j.1365-2958.2011.07710.x.
3. **Pathak DT, Wei X, Bucuvalas A, Haft DH, Gerloff DL, Wall D.** 2012. Cell contact-dependent outer membrane exchange in myxobacteria: genetic determinants and mechanism. PLoS Genet. **8:**e1002626. http://dx.doi.org/10.1371/journal.pgen.1002626.
4. **Pathak DT, Wall D.** 2012. Identification of the *cglC*, *cglD*, *cglE*, and *cglF* genes and their role in cell contact-dependent gliding motility in *Myxococcus xanthus*. J. Bacteriol. **194:**1940–1949. http://dx.doi.org/10.1128/JB.00055-12.
5. **Hodgkin J, Kaiser D.** 1977. Cell-to-cell stimulation of movement in nonmotile mutants of *Myxococcus*. Proc. Natl. Acad. Sci. U. S. A. **74:**2938–2942. http://dx.doi.org/10.1073/pnas.74.7.2938.
6. **Bhat S, Zhu X, Patel RP, Orlando R, Shimkets LJ.** 2011. Identification and localization of *Myxococcus xanthus* porins and lipoproteins. PLoS One **6:**e27475. http://dx.doi.org/10.1371/journal.pone.0027475.
7. **Wall D.** 2014. Molecular recognition in myxobacterial outer membrane exchange: functional, social and evolutionary implications. Mol. Microbiol. **91:**209–220. http://dx.doi.org/10.1111/mmi.12450.
8. **Rodriguez-Soto JP, Kaiser D.** 1997. The *tgl* gene: social motility and stimulation in *Myxococcus xanthus*. J. Bacteriol. **179:**4361–4371.
9. **Rodriguez AM, Spormann AM.** 1999. Genetic and molecular analysis of *cglB*, a gene essential for single-cell gliding in *Myxococcus xanthus*. J. Bacteriol. **181:**4381–4390.
10. **Nan B, Zusman DR.** 2011. Uncovering the mystery of gliding motility in the myxobacteria. Annu. Rev. Genet. **45:**21–39. http://dx.doi.org/10.1146/annurev-genet-110410-132547.
11. **Nan B, McBride MJ, Chen J, Zusman DR, Oster G.** 2014. Bacteria that glide with helical tracks. Curr. Biol. **24:**R169–R173. http://dx.doi.org/10.1016/j.cub.2013.12.034.
12. **Wall D, Kaiser D.** 1999. Type IV pili and cell motility. Mol. Microbiol. **32:**1–10. http://dx.doi.org/10.1046/j.1365-2958.1999.01339.x.
13. **Pathak DT, Wei X, Dey A, Wall D.** 2013. Molecular recognition by a polymorphic cell surface receptor governs cooperative behaviors in bacteria. PLoS Genet. **9:**e1003891. http://dx.doi.org/10.1371/journal.pgen.1003891.
14. **Pathak DT, Wei X, Wall D.** 2012. Myxobacterial tools for social interactions. Res. Microbiol. **163:**579–591. http://dx.doi.org/10.1016/j.resmic.2012.10.022.
15. **Wall D, Kaiser D.** 1998. Alignment enhances the cell-to-cell transfer of pilus phenotype. Proc. Natl. Acad. Sci. U. S. A. **95:**3054–3058. http://dx.doi.org/10.1073/pnas.95.6.3054.
16. **Wall D, Kolenbrander PE, Kaiser D.** 1999. The *Myxococcus xanthus pilQ* (*sglA*) gene encodes a secretin homolog required for type IV pilus biogenesis, social motility, and development. J. Bacteriol. **181:**24–33.
17. **Larsen RA, Wilson MM, Guss AM, Metcalf WW.** 2002. Genetic analysis of pigment biosynthesis in *Xanthobacter autotrophicus* Py2 using a new, highly efficient transposon mutagenesis system that is functional in a wide variety of bacteria. Arch. Microbiol. **178:**193–201. http://dx.doi.org/10.1007/s00203-002-0442-2.
18. **Youderian P, Burke N, White DJ, Hartzell PL.** 2003. Identification of genes required for adventurous gliding motility in *Myxococcus xanthus* with the transposable element mariner. Mol. Microbiol. **49:**555–570. http://dx.doi.org/10.1046/j.1365-2958.2003.03582.x.
19. **Julien B, Kaiser AD, Garza A.** 2000. Spatial control of cell differentiation in *Myxococcus xanthus*. Proc. Natl. Acad. Sci. U. S. A. **97:**9098–9103. http://dx.doi.org/10.1073/pnas.97.16.9098.
20. **Nudleman E, Wall D, Kaiser D.** 2006. Polar assembly of the type IV pilus secretin in *Myxococcus xanthus*. Mol. Microbiol. **60:**16–29. http://dx.doi.org/10.1111/j.1365-2958.2006.05095.x.
21. **Mori Y, Maeda M, Takegawa K, Kimura Y.** 2012. PhpA, a tyrosine phosphatase of *Myxococcus xanthus*, is involved in the production of exopolysaccharide. Microbiology **158:**2546–2555. http://dx.doi.org/10.1099/mic.0.059824-0.
22. **Lu A, Cho K, Black WP, Duan XY, Lux R, Yang Z, Kaplan HB, Zusman DR, Shi W.** 2005. Exopolysaccharide biosynthesis genes required for social motility in *Myxococcus xanthus*. Mol. Microbiol. **55:**206–220. http://dx.doi.org/10.1111/j.1365-2958.2004.04369.x.
23. **Shi W, Zusman DR.** 1993. The two motility systems of *Myxococcus xanthus* show different selective advantages on various surfaces. Proc. Natl. Acad. Sci. U. S. A. **90:**3378–3382. http://dx.doi.org/10.1073/pnas.90.8.3378.
24. **Ernst CM, Peschel A.** 2011. Broad-spectrum antimicrobial peptide resistance by MprF-mediated aminoacylation and flipping of phospholipids. Mol. Microbiol. **80:**290–299. http://dx.doi.org/10.1111/j.1365-2958.2011.07576.x.
25. **Krogh A, Larsson B, von Heijne G, Sonnhammer EL.** 2001. Predicting transmembrane protein topology with a hidden Markov model: applica-

tion to complete genomes. J. Mol. Biol. **305:**567–580. http://dx.doi.org/10.1006/jmbi.2000.4315.
26. **Finn RD, Bateman A, Clements J, Coggill P, Eberhardt RY, Eddy SR, Heger A, Hetherington K, Holm L, Mistry J, Sonnhammer EL, Tate J, Punta M.** 2014. Pfam: the protein families database. Nucleic Acids Res. **42:**D222–D230. http://dx.doi.org/10.1093/nar/gkt1223.
27. **Goldman BS, Nierman WC, Kaiser D, Slater SC, Durkin AS, Eisen JA, Ronning CM, Barbazuk WB, Blanchard M, Field C, Halling C, Hinkle G, Iartchuk O, Kim HS, Mackenzie C, Madupu R, Miller N, Shvartsbeyn A, Sullivan SA, Vaudin M, Wiegand R, Kaplan HB.** 2006. Evolution of sensory complexity recorded in a myxobacterial genome. Proc. Natl. Acad. Sci. U. S. A. **103:**15200–15205. http://dx.doi.org/10.1073/pnas.0607335103.
28. **Jamsheer K M, Laxmi A.** 2014. DUF581 is plant specific FCS-like zinc finger involved in protein-protein interaction. PLoS One **9:**e99074. http://dx.doi.org/10.1371/journal.pone.0099074.
29. **Sengupta S, Nagaraja V.** 2008. YacG from *Escherichia coli* is a specific endogenous inhibitor of DNA gyrase. Nucleic Acids Res. **36:**4310–4316. http://dx.doi.org/10.1093/nar/gkn355.
30. **Markowitz VM, Chen IM, Palaniappan K, Chu K, Szeto E, Pillay M, Ratner A, Huang J, Woyke T, Huntemann M, Anderson I, Billis K, Varghese N, Mavromatis K, Pati A, Ivanova NN, Kyrpides NC.** 2014. IMG 4 version of the integrated microbial genomes comparative analysis system. Nucleic Acids Res. **42:**D560–D567. http://dx.doi.org/10.1093/nar/gkt963.
31. **Cascales E, Christie PJ.** 2003. The versatile bacterial type IV secretion systems. Nat. Rev. Microbiol. **1:**137–149. http://dx.doi.org/10.1038/nrmicro753.
32. **Konovalova A, Petters T, Sogaard-Andersen L.** 2010. Extracellular biology of *Myxococcus xanthus*. FEMS Microbiol. Rev. **34:**89–106. http://dx.doi.org/10.1111/j.1574-6976.2009.00194.x.
33. **Hayes CS, Koskiniemi S, Ruhe ZC, Poole SJ, Low DA.** 2014. Mechanisms and biological roles of contact-dependent growth inhibition systems. Cold Spring Harb. Perspect. Med. **4:**a010025. http://dx.doi.org/10.1101/cshperspect.a010025.
34. **Martens S, McMahon HT.** 2008. Mechanisms of membrane fusion: disparate players and common principles. Nat. Rev. Mol. Cell Biol. **9:**543–556. http://dx.doi.org/10.1038/nrm2417.
35. **Wei X, Vassallo CN, Pathak DT, Wall D.** 2014. Myxobacteria produce outer membrane-enclosed tubes in unstructured environments. J. Bacteriol. **196:**1807–1814. http://dx.doi.org/10.1128/JB.00850-13.
36. **Hartzell T.** 2014. All in the family: kin contact leads to outer membrane exchange. J. Bacteriol. **196:**1789–1792. http://dx.doi.org/10.1128/JB.01617-14.
37. **Kaiser D, Warrick H.** 2014. Transmission of a signal that synchronizes cell movements in swarms of *Myxococcus xanthus*. Proc. Natl. Acad. Sci. U. S. A. **111:**13105–13110. http://dx.doi.org/10.1073/pnas.1411925111.
38. **Roy H, Ibba M.** 2009. Broad range amino acid specificity of RNA-dependent lipid remodeling by multiple peptide resistance factors. J. Biol. Chem. **284:**29677–29683. http://dx.doi.org/10.1074/jbc.M109.046367.
39. **Arendt W, Hebecker S, Jager S, Nimtz M, Moser J.** 2012. Resistance phenotypes mediated by aminoacyl-phosphatidylglycerol synthases. J. Bacteriol. **194:**1401–1416. http://dx.doi.org/10.1128/JB.06576-11.
40. **Slavetinsky CJ, Peschel A, Ernst CM.** 2012. Alanyl-phosphatidylglycerol and lysyl-phosphatidylglycerol are translocated by the same MprF flippases and have similar capacities to protect against the antibiotic daptomycin in *Staphylococcus aureus*. Antimicrob. Agents Chemother. **56:**3492–3497. http://dx.doi.org/10.1128/AAC.00370-12.
41. **Ernst CM, Staubitz P, Mishra NN, Yang SJ, Hornig G, Kalbacher H, Bayer AS, Kraus D, Peschel A.** 2009. The bacterial defensin resistance protein MprF consists of separable domains for lipid lysinylation and antimicrobial peptide repulsion. PLoS Pathog. **5:**e1000660. http://dx.doi.org/10.1371/journal.ppat.1000660.
42. **Roy H, Dare K, Ibba M.** 2009. Adaptation of the bacterial membrane to changing environments using aminoacylated phospholipids. Mol. Microbiol. **71:**547–550. http://dx.doi.org/10.1111/j.1365-2958.2008.06563.x.
43. **Curtis PD, Geyer R, White DC, Shimkets LJ.** 2006. Novel lipids in *Myxococcus xanthus* and their role in chemotaxis. Environ. Microbiol. **8:**1935–1949. http://dx.doi.org/10.1111/j.1462-2920.2006.01073.x.
44. **Roy H.** 2009. Tuning the properties of the bacterial membrane with aminoacylated phosphatidylglycerol. IUBMB Life **61:**940–953. http://dx.doi.org/10.1002/iub.240.